Observation of the Fermi surface, the band structure, and their diffraction replicas of $Sr_{14-x}Ca_xCu_{24}O_{41}$ by angle-resolved photoemission spectroscopy

A. Koitzsch,[1] D. S. Inosov,[1,2] H. Shiozawa,[1,3] V. B. Zabolotnyy,[1] S. V. Borisenko,[1] A. Varykhalov,[4] C. Hess,[1] M. Knupfer,[1] U. Ammerahl,[5] A. Revcolevschi,[5] and B. Büchner[1]

[1]*Institute for Solid State Research, IFW-Dresden, P.O. Box 270116, D-01171 Dresden, Germany*

[2]*Max-Planck-Institute for Solid State Research, Heisenbergstraße 1, D-70569 Stuttgart, Germany*

[3]*Advanced Technology Institute, University of Surrey, Guildford GU2 7XH, United Kingdom*

[4]*BESSY GmbH, Albert-Einstein-Strasse 15, 12489 Berlin, Germany*

[5]*Laboratoire de Physico-Chimie de l'État Solide, Université Paris-Sud, 91405 Orsay, France*

(Received 1 February 2010; published 29 March 2010)

We have investigated the electronic structure of $Sr_{14-x}Ca_xCu_{24}O_{41}$ ($x=0$; 11.5) single crystals by angle-resolved photoemission spectroscopy. A satisfactory agreement with band-structure calculations is found. The Fermi surface is observed for $Sr_{2.5}Ca_{11.5}Cu_{24}O_{41}$ from which we derive a charge carrier concentration between 0.15 and 0.2 holes per Cu atom at $T=25$ K in the ladder substructure. The chain substructures, on the other hand, act as diffraction grating for the ladder photoelectrons giving rise to incommensurate replicas of the ladder bands.

DOI: 10.1103/PhysRevB.81.113110 PACS number(s): 71.20.−b

Cuprate two-leg ladder compounds of the type $Sr_{14-x}Ca_xCu_{24}O_{41}$ have been in the focus of intense research for many reasons: (i) they are believed to be relevant for the cuprate high-T_c problem, both as simpler paradigm of *t-J* models[1] and due to the known affinity of the two-dimensional cuprates to one-dimensional (stripe) phenomena;[2] (ii) as quasi-one-dimensional materials they are subject to strong quantum fluctuations and complex density wave order giving rise to exotic ground states;[3] (iii) they are superconductors in their own right with an unresolved pairing mechanism.[4]

The $Sr_{14-x}Ca_xCu_{24}O_{41}$ systems possess a complicated crystal structure consisting of alternating layers of ladder and chain planes. Since the principal building units of both structures, the CuO_4 plaquettes, are rotated by 45° with respect to each other, their lattice constant c_L (ladder) and c_C (chain) have a ratio of $\sqrt{2}$ and are, hence, incommensurate.

It is a disturbing situation that, in spite of intense efforts, no consensus could be reached on a basic property of the ladder structure, namely, its charge content. The nominal charge count gives six holes per formula unit when counted from a Cu^{2+} state for $Sr_{14}Cu_{24}O_{41}$. However, it has proven to be difficult to ascertain how the charge is distributed among ladders and chains. Values from 1.1 hole [corresponding to 0.08 holes per ladder (h.p.l.) Cu^{2+}] (Ref. 5), 2.8 (0.2 h.p.l. Cu^{2+}) holes,[6] to 4.4 (0.31 h.p.l. Cu^{2+}) holes[7] among many others are reported for $Sr_{11-12}Ca_{3-2}Cu_{24}O_{41}$ with no sign of convergence with time. Ca substitution does not dope the system but exerts chemical pressure on the lattice causing a hole transfer to the ladder. The charge balance between ladders and chains is also affected by temperature and external pressure, which is a precondition for superconductivity. Both chains and ladders are prone to charge order, the specific type of which depends on the carrier concentration.

Detailed knowledge of the low-energy electronic structure is lacking so far. A previous angle-resolved photoemission spectroscopy (ARPES) study of $Sr_{14}Cu_{24}O_{41}$ (Ref. 8) found signatures of dispersing features obeying the expected ladder periodicity. Recently, two-dimensional momentum distribution maps have been made available[9] indicating a quasi-one-dimensional behavior of the ladders. However, the data quality does not allow stringent conclusions on crucial aspects so far: which paradigm governs the ladders, one-particle band-structure calculations, or theories explicitly taking into account correlation effects? How does the Fermi surface (FS) look like for the metallic samples and what charge content can be derived from it?

Here we resolve a number of the uncertainties mentioned above. In particular, we compare the ARPES spectra taken from $Sr_{14-x}Ca_xCu_{24}O_{41}$ ($x=0$; 11.5) to local-density approximation (LDA) based band-structure calculations and find remarkable agreement.[10,11] We measure the Fermi surface of $Sr_{2.5}Ca_{11.5}Cu_{24}O_{41}$ and obtain the hole content from its volume taking advantage of the fact that the chain bands do not reach E_F (Fermi energy). Nevertheless, the complex crystal structure severely affects the spectra. It entails the appearance of diffraction replicas similar to those of other cuprate systems.

Experiments have been performed at BESSY ("1^3 station") with a photon energy of $h\nu=100$ eV. The energy resolution was 25 meV or better; the momentum resolution was 0.02 $Å^{-1}$. The crystals were grown by the traveling solvent floating zone method.[12]

We start the presentation of the results with $Sr_{14}Cu_{24}O_{41}$. Figure 1(a) shows the angle-integrated valence band. Its shape agrees with previous publications.[8] At low binding energies a foot structure is observed, which does not extend up to the Fermi energy. This indicates the presence of a gap in agreement with the nonmetallic nature of $Sr_{14}Cu_{24}O_{41}$.[13] It is the energy region highlighted by the dashed rectangle we are mainly interested in. Inspection of the angle-resolved photoemission intensity reveals dispersive features which generally yield well-defined peaks along the momentum axes [i.e., in the momentum distribution curves (MDCs)] but not along the energy axes [i.e., in the energy distribution curves (EDCs)]. Figure 1(c) depicts the distribution of photoemis-

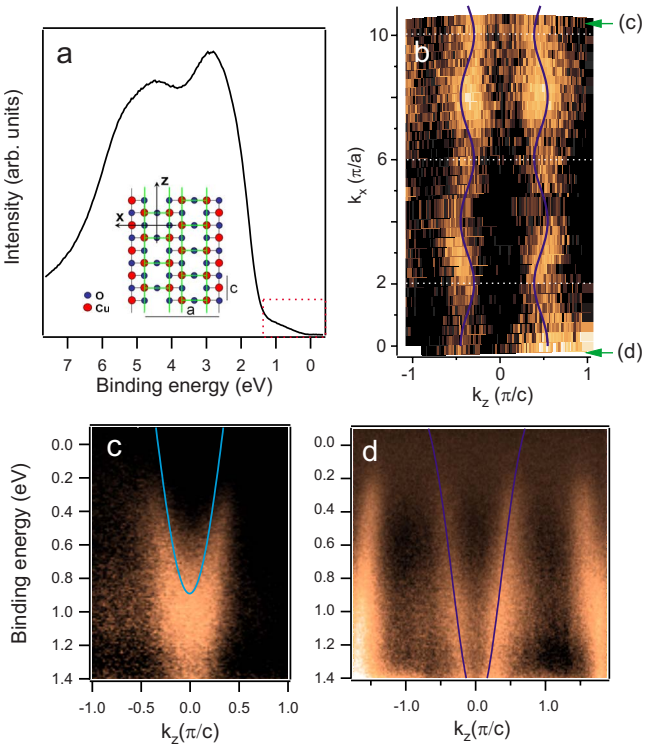

FIG. 1. (Color online) Photoemission spectra of $Sr_{14}Cu_{24}O_{41}$ taken at room temperature with $h\nu=100$ eV. (a) k-integrated valence band. The dispersive features in panels (b)–(d) appear on top of the smooth tail of the valence band highlighted by the dashed rectangle. Inset: crystal structure of the ladder plane. (b) Momentum distribution map of photoemission intensity at $E_B=0.4$ eV integrated over $\Delta E=0.08$ eV taken with the light polarization parallel to the ladder direction. The blue line corresponds to the tight-binding (tb) fit of LDA band-structure calculations from Ref. 10 for the bonding band. The latter is also depicted in panel (d). Green arrows mark the k_x positions of the measurements in (c) and (d). (c) EDM with perpendicular polarization. Smooth background intensity from the main valence band has been subtracted. The light blue line corresponds to the antibonding band of Ref. 10. (d) Energy distribution map taken with parallel polarization compared to tb band.

sion intensity as a function of binding energy and momentum along the ladder direction [energy distribution map (EDM)]. A band symmetric to the Γ point is observed with a bandwidth of ~ 1 eV. It has a strong intensity around $E_B=1$ eV which rapidly decreases for lower binding energies. This band can be assigned to ladder states for the following reasons: (i) it has the periodicity of the ladder; (ii) no large dispersion is expected for the chain structure, which is, from an electronic point of view, a quasi-zero-dimensional object. This assignment is further corroborated by the comparison with LDA based band-structure calculations. The light blue line corresponds to the tight-binding form derived by Arai *et al.* for the antibonding band for the ladder states. The tight-binding parameters have been taken from Ref. 10 for $Sr_{14}Cu_{24}O_{41}$ without any modification. The agreement is satisfactory but could be further improved by a slight downshift of the blue curve. The data in Fig. 1(c) have been measured with a polarization of the incoming light perpendicular to the ladder direction at a fixed k_x value. Figure 1(d) shows a similar data set but at different k_x and with parallel polarization. The obtained spectra show clear differences with Fig. 1(c). In particular, the bandwidth is increased and the two branches of the band symmetric to Γ are more clearly separated. Again, this band has the periodicity of the ladder plane. It fits very well to the bonding band (blue line) with the same parameter set as in Fig. 1(c). Obviously, the bands are very efficiently suppressed/enhanced by the polarization conditions due to the influence of the photoemission matrix element. The diffuse intensity around $E_B=1$ eV stems from the weakly dispersing chain bands. This is also seen in Fig. 1(c) and as a small peak at $E_B=1$ eV in Fig. 1(a). The intensity of the band fades away when approaching the gap with no sign of backdispersion. Figure 1(b) presents the photoemission intensity at $E_B=0.4$ eV as a function of k_z and k_x with the same polarization as in Fig. 1(d). The band discloses its quasi-one-dimensional character which is, however, modulated due to the interladder interaction. Again, the agreement with the band-structure calculations is convincing. The parameters for the tight-binding form are identical to Figs. 1(c) and 1(d).

The LDA calculations give an adequate description of the low-energy electronic structure—except for the appearance of the gap. If the gap was Mott-Hubbard-like, renormalizations of the bandwidth and shape would be expected but are not observed. Therefore, the most likely explanation for the insulating ground state is a low-energy phenomenon such as a charge-density wave proposed previously.[13,14] The fact that we do not observe backfolded bands may be related to weak backfolding potentials.

Now we proceed to the Ca-substituted sample. Figure 2(a) shows an EDM equivalent to that of Fig. 1(c), i.e., with perpendicular polarization. Similar to Figs. 1(c) and 1(d) a "V"-shaped band, symmetric to Γ, is observed. Additionally, two bands at higher momenta appear. They are identical but mirrored with respect to the main bands. The intensity of the bands is cut off by the Fermi energy signaling metallic behavior. Compared to $Sr_{14}Cu_{24}O_{41}$ the features have sharpened significantly. The blue line is essentially identical to the one in Fig. 1(c) giving again convincing agreement between experiment and theory. Upon Ca substitution, holes are transferred to the ladder effectively shifting the ladder bands up. The fact that the experimental band fits the theoretical band in Fig. 2(a) well, whereas it appears somewhat downshifted in Fig. 1(c), confirms this conjecture. What is the origin of the additional bands? Certainly they are not predicted by the LDA. The fact that they appear to be (momentum) shifted replicas of the principal bands suggests that they originate from some modulation of the original crystal structure (due to, e.g., charge order) or from extrinsic diffraction. Extrinsic means here that the photoelectrons can be diffracted when they leave the sample, a well known effect, e.g., for $Bi_2Sr_2CaCu_2O_8$.[15] The Ca content of our sample is close to $x=11$ for which a charge-density wave with $Q=2/3\ \pi/c_L$ was reported in Ref. 16. However, this vector does not match the distance between the replica and main bands, which is incommensurate with the ladder lattice [see Figs. 2(c) and 2(d)]. To get more insight we study the Fermi surface map in Fig. 2(b). The principal bands fit to the calculations. The additional bands are also clearly visible and situated close to

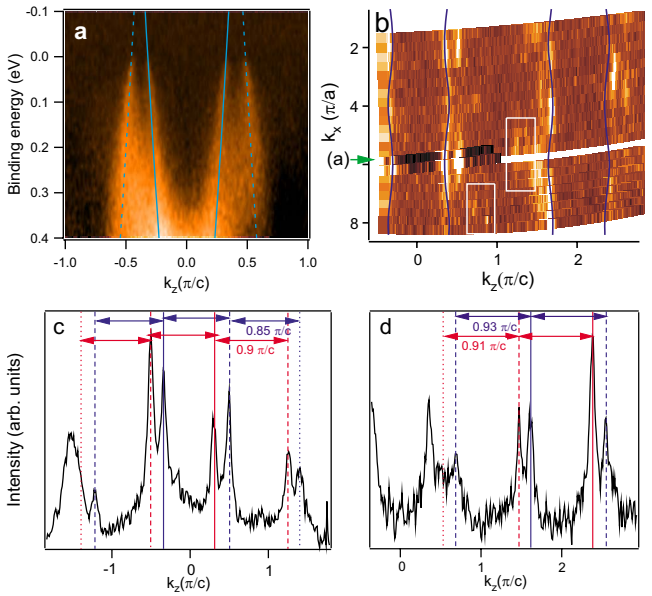

FIG. 2. (Color online) Electronic structure of $Sr_{2.5}Ca_{11.5}Cu_{24}O_{41}$ measured with photon energy $h\nu=100$ eV at $T=25$ K with perpendicular polarization. (a) EDM parallel to k_z with perpendicular polarization. Smooth background intensity from the main valence band has been subtracted. The blue line corresponds to the calculated antibonding band of Ref. 10 and is equivalent to the light blue line of Fig. 1(c). The dashed lines are copies of the main band shifted along the k axes. (b) Fermi surface map obtained by integrating spectral intensity in the range $E=0-35$ meV. The blue lines indicate again the band-structure calculation with the same parameters as in (a). The white rectangles highlight regions with possible higher order diffraction replicas. The green arrow marks the k_x position of (a). [(c) and (d)] Momentum distribution curves parallel to k_z. Solid lines indicate principle bands, dashed lines their first, and dotted lines their second replica. The arrows of the same color in each panel have equal lengths.

the main bands. However, there are more features to be observed in the map. Two examples are highlighted by the white rectangles. It seems that weak replicas of both principal and additional bands appear in these regions. A reasonable assumption is that these are higher order diffraction replicas. Figures 2(c) and 2(d) present MDC covering a large k_z interval. It is clear from these figures that the peaks can be classified as zero, first, and second diffraction replicas, with an average vector of $Q=0.9\ \pi/c_L$. This vector is within error bars equal to the difference between principal ladder and chain periodicity: $Q=2\pi/c_C-2\pi/c_L=0.88\pi/c_L$. This reveals the origin of the additional bands as diffraction replicas of the main bands imposed by the scattering of the photoelectrons by the incommensurate chain structure. This assignment is corroborated by the polarization dependence of the features: if we switch the polarization to parallel (not shown), the intensities of both main bands and replicas are equally suppressed indicating symmetry related wave functions. (Unlike for the Ca-free sample, the bonding band is, however, not strongly enhanced in this case resulting in overall weak intensity.) Alternative explanations for the appearance of the replicas include a possible structural distortion of the ladder plane imposed by the chains or a CDW order with

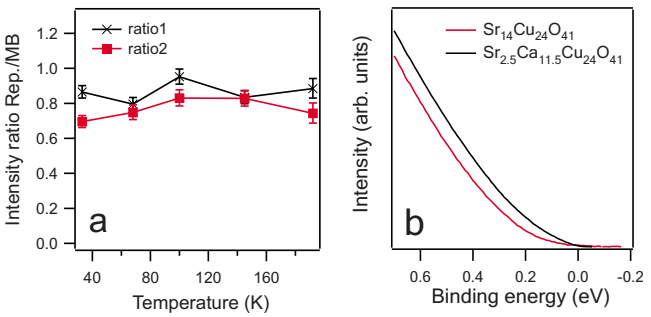

FIG. 3. (Color online) (a) Intensity ratio of main band (MB) and replica for left and right halves (ratios 1 and 2) of the Brillouin zone as a function of temperature. Intensities are obtained from Lorentzian fitting of MDC cuts. (b) Low-energy angle-integrated spectral weight for $Sr_{14}Cu_{24}O_{41}$ and $Sr_{2.5}Ca_{11.5}Cu_{24}O_{41}$ (without background subtraction).

suitable periodicity. However, from neutron-diffraction refinement it is known that the structural modulations of the ladder are small,[17] which implies weak backfolding potential and, hence, weak spectral weight of the replicas.[18] In contrast, we observe comparable intensities for the main band and replica. A CDW scenario becomes unlikely due to the absence of a sizable temperature dependence of the intensity ratio of the main bands and diffraction replica (Fig. 3) as would be expected for a charge-density wave.

No diffraction replicas are, however, observed for $Sr_{14}Cu_{24}O_{41}$. To explain this we argue that the features are broad for $Sr_{14}Cu_{24}O_{41}$ and quite strongly suppressed near E_F where the replicas are best seen in $Sr_{2.5}Ca_{11.5}Cu_{24}O_{41}$. In essence, they are probably too weak to be observed at this stage.

From the volume of the Fermi surface in Fig. 2(b) the charge carrier density can be obtained according to $1+\delta=2\cdot S_{FS}/S_{BZ}$, where δ is the number of holes, S_{FS} is the volume of the hole FS, and S_{BZ} is the volume of the Brillouin zone. Applying this formula to Fig. 2(b) and using the tight-binding fit to evaluate the volume, we obtain a hole count of $\delta_{ab}=0.3$. However, the invisible bonding band has to be taken into account as well. From Fig. 1 we concluded that the LDA somewhat overestimates the energy splitting of the bonding and antibonding bands. To quantify this observation we extracted the experimental dispersion from the data in Figs. 1(c) and 1(d) by fitting Lorentzians to the MDC cuts. Then the tight-binding form was fitted to the experimental dispersion with the energy offset as the only adjustable parameter. In this way a shift of bonding and antibonding bands of $\Delta E=260$ meV toward each other relative to the LDA calculation was extracted. For the evaluation of δ_{bb} we used the corresponding bonding tight-binding band at $E=0$ but shifted up in energy by ΔE. We obtain $\delta_{bb}=0.1$. The total hole count sums up to $\delta=0.4$ for the ladder unit cell or to $\delta=0.2$ holes per ladder Cu^{2+}. The main source of error for this value comes from a possible doping dependence of the splitting. To estimate this error we refer again to the LDA calculation and compare the difference of the splitting at $k_z=0$ and $k_x=0$ for $Sr_{14}Cu_{24}O_{41}$ and $Ca_{14}Cu_{24}O_{41}$.[10] The splitting is 140 meV larger for the fully calcium-substituted compound. For the present situation this shifts the bonding band downward with

respect to the antibonding band and reduces the number of holes resulting in $\delta=0.15$ holes per ladder Cu^{2+}. The real value of δ lies in between 0.15 and 0.2 holes per ladder Cu^{2+}.

Our value for the hole content is larger than the one previously extracted from x-ray absorption spectroscopy data[5] but too small to sustain the charge-density wave observed in Ref. 16. Note, however, that the Fermi surface takes into account only the metallic holes. The fact that the Fermi surface volume of $Sr_{14}Cu_{24}O_{41}$ is zero (because it is insulating) does not mean that no holes are present, but rather that they are localized. Localization effects (or, more specifically, CDW fluctuations) may also be present in $Sr_{2.5}Ca_{11.5}Cu_{24}O_{41}$ as indicated by the absence of the Fermi edge in Fig. 3(b) (Ref. 9). This pseudogaplike suppression of spectral weight near E_F is often observed in the realm of charge order.[19] An alternative explanation, however, could be the one-dimensional nature of the ladder structure. The density of states for the Luttinger liquid is suppressed compared to the Fermi liquid.

In summary, we investigated the electronic structure of $Sr_{14}Cu_{24}O_{41}$ by ARPES. The results are generally well described by LDA-type band-structure calculations. From the FS map of $Sr_{2.5}Ca_{11.5}Cu_{24}O_{41}$ we obtain a charge content δ between 0.15 and 0.2 holes per Cu for the ladder. The chain layers act as diffraction gratings for the ladders. No direct fingerprints of charge-density waves are observed, but certain aspects of the data such as the gap in $Sr_{14}Cu_{24}O_{41}$ or the absence of a Fermi edge in $Sr_{2.5}Ca_{11.5}Cu_{24}O_{41}$ are consistent with the presence of CDW fluctuations.

ACKNOWLEDGMENTS

We acknowledge technical assistance by R. Hübel, R. Schönfelder and S. Leger.

[1] E. Dagotto, J. Riera, and D. Scalapino, Phys. Rev. B **45**, 5744 (1992).
[2] J. M. Tranquada, B. J. Sternlieb, J. D. Axe, Y. Nakamura, and S. Uchida, Nature (London) **375**, 561 (1995).
[3] T. Vuletic, B. Korin-Hamzić, T. Ivek, S. Tomić, B. Gorshunov, M. Dressel, and J. Akimitsu, Phys. Rep. **428**, 169 (2006).
[4] M. Uehara, T. Nagata, J. Akimitsu, H. Takahashi, N. Môri, and K. Kinoshita, J. Phys. Soc. Jpn. **65**, 2764 (1996).
[5] N. Nücker, M. Merz, C. A. Kuntscher, S. Gerhold, S. Schuppler, R. Neudert, M. S. Golden, J. Fink, D. Schild, S. Stadler, V. Chakarian, J. Freeland, Y. U. Idzerda, K. Conder, M. Uehara, T. Nagata, J. Goto, J. Akimitsu, N. Motoyama, H. Eisaki, S. Uchida, U. Ammerahl, and A. Revcolevschi, Phys. Rev. B **62**, 14384 (2000).
[6] T. Osafune, N. Motoyama, H. Eisaki, and S. Uchida, Phys. Rev. Lett. **78**, 1980 (1997).
[7] A. Rusydi, M. Berciu, P. Abbamonte, S. Smadici, H. Eisaki, Y. Fujimaki, S. Uchida, M. Rübhausen, and G. A. Sawatzky, Phys. Rev. B **75**, 104510 (2007).
[8] T. Takahashi, T. Yokoya, A. Ashihara, O. Akaki, H. Fujisawa, A. Chainani, M. Uehara, T. Nagata, J. Akimitsu, and H. Tsunetsugu, Phys. Rev. B **56**, 7870 (1997).
[9] T. Yoshida, X. J. Zhou, Z. Hussain, Z.-X. Shen, A. Fujimori, H. Eisaki, and S. Uchida, Phys. Rev. B **80**, 052504 (2009).
[10] M. Arai and H. Tsunetsugu, Phys. Rev. B **56**, R4305 (1997).
[11] T. F. A. Müller, V. Anisimov, T. M. Rice, I. Dasgupta, and T. Saha-Dasgupta, Phys. Rev. B **57**, R12655 (1998).
[12] U. Ammerahl, G. Dhalenne, A. Revcolevschi, J. Berthon, and H. Moudden, J. Cryst. Growth **193**, 55 (1998).
[13] C. Hess, H. ElHaes, B. Büchner, U. Ammerahl, M. Hücker, and A. Revcolevschi, Phys. Rev. Lett. **93**, 027005 (2004).
[14] G. Blumberg, P. Littlewood, A. Gozar, B. S. Dennis, N. Motoyama, H. Eisaki, and S. Uchida, Science **297**, 584 (2002).
[15] H. Ding, A. F. Bellman, J. C. Campuzano, M. Randeria, M. R. Norman, T. Yokoya, T. Takahashi, H. Katayama-Yoshida, T. Mochiku, K. Kadowaki, G. Jennings, and G. P. Brivio, Phys. Rev. Lett. **76**, 1533 (1996).
[16] A. Rusydi, P. Abbamonte, H. Eisaki, Y. Fujimaki, G. Blumberg, S. Uchida, and G. A. Sawatzky, Phys. Rev. Lett. **97**, 016403 (2006).
[17] J. Etrillard, M. Braden, A. Gukasov, U. Ammerahl, and A. Revcolevschi, Physica C **403**, 290 (2004).
[18] J. Voit, L. Perfetti, F. Zwick, H. Berger, G. Margaritondo, G. Grüner, H. Höchst, and M. Grioni, Science **290**, 501 (2000).
[19] S. V. Borisenko, A. A. Kordyuk, A. N. Yaresko, V. B. Zabolotnyy, D. S. Inosov, R. Schuster, B. Büchner, R. Weber, R. Follath, L. Patthey, and H. Berger, Phys. Rev. Lett. **100**, 196402 (2008).